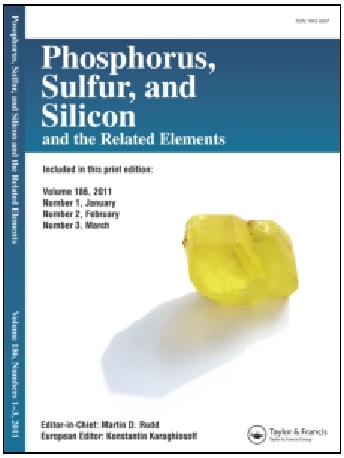

Phosphorus, Sulfur, and Silicon and the Related Elements
Publication details, including instructions for authors and subscription information:
http://www.informaworld.com/smpp/title~content=t713618290

Temperature Dependence of the Electrical Conductivity of Cyclodiphosph(V)azane Derivative and Its Copper (II) Complex

A. M. A. Alaghaz[a]; S. M. Shaaban[a]
[a] Chemistry Department, Faculty of Science (Boys), Al-Azhar University, Nasr City, Cairo, Egypt

To cite this Article Alaghaz, A. M. A. and Shaaban, S. M.(2008) 'Temperature Dependence of the Electrical Conductivity of Cyclodiphosph(V)azane Derivative and Its Copper (II) Complex', Phosphorus, Sulfur, and Silicon and the Related Elements, 183: 10, 2464 — 2475

To link to this Article: DOI: 10.1080/10426500801964028

URL: http://dx.doi.org/10.1080/10426500801964028

Phosphorus, Sulfur, and Silicon, 183:2464–2475, 2008
Copyright © Taylor & Francis Group, LLC
ISSN: 1042-6507 print / 1563-5325 online
DOI: 10.1080/10426500801964028

Temperature Dependence of the Electrical Conductivity of Cyclodiphosph(V)azane Derivative and Its Copper (II) Complex

A. M. A. Alaghaz and S. M. Shaaban
Chemistry Department, Faculty of Science (Boys), Al-Azhar University, Nasr City, Cairo, Egypt

Correlation of the current-voltage and temperature dependence of the electrical conductivity with the molecular structure data including infrared and ultraviolet spectra of ligand [2,2,4,4-tetrachloro-1,3-diphenyl-2,4-bi(5-imino-4-cyano-3-methylthiopyazo-1-yl-methylcarbodi-thioate)cyclodiphosph(V)zane and its copper complex have been investigated. The result of the electrical conductivity, energy gaps obtained from electrical conductivity in the solid state was consistent with those of semiconductor materials.

Keywords Cyclodiphosph(V)azane ring and its copper (II) complex; electrical conductivity; temperature dependence

INTRODUCTION

In the last decades, great efforts have been devoted to studying the relationship between the structure of inorganic and organic compounds and their electrical properties.[1–7] The electrical conductivity of different complexes of organic phosphorus compounds and their properties to the chemical structure have been investigated.[8,9] In the present work, D. C. conductivity properties of new synthesized cyclodiphosph(V)azane with 5-amino-4-cyano-3-methylthio-pyrazo-1-yl-methyl carbodit-hioate and its copper (II) complex, as well as relating these properties to the chemical structure, have been carried out.

Received 10 February 2007; accepted 14 December 2007.

Address correspondence to A. M. A. Alaghaz, Chemistry Department, Faculty of Science (Boys), Al-Azhar University, Nasr-City, Cairo, Egypt. E-mail: aalajhaz@hotmail.com

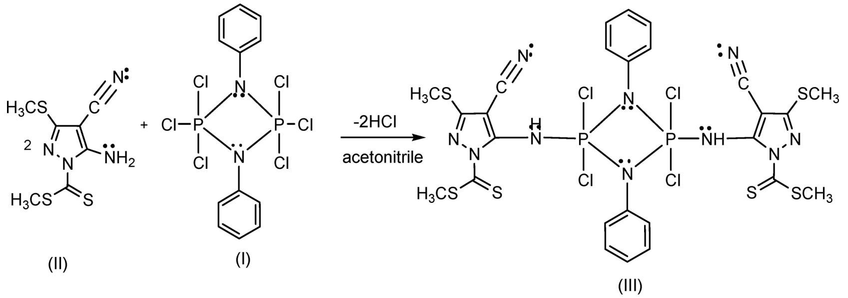

SCHEME 1 Molecular configuration of the ligand (1,3-diphenyl-,2,2, ,4,4-tetrachloro-bis(5-imino-4-cyano-3-methylthiopyrazo-1-yl-methylcarbodithioate) cyclodiphosph(V)azane.

EXPERIMENTAL

The ligand Scheme 1 is prepared by the reaction of 1,3-diphenyl-2,2,2,4,4,4-hexachlorocyclodiphosph(V)azane with the solid of 5-amino-4-cyano-3-methylthio-pyrazo-1-yl-methylcarbodithioate(II) (2.49 g, 0.01 mmol) was added in small portions to a well-stirred solution hexachlorocyclodiphosph(V)azane (I) (2.29 g, 0.005 mmol) in 100 ml acetonitrile over a half-hour period. After the complete addition, the reaction mixture was heated under reflux for 2 h with continuous stirring. After completion of the reaction (HCl gas ceased to evolve), the reaction mixture was filtered while hot and the filtrate was left to cool at room temperature. The obtained solid was filtered, washed several times with acetonitril, and dried in vacuo to give the corresponding aminocyclodiphosph(V)azane (III) derivative. The purity of the aminocyclodiphosph(V)azane derivative (ligand) was confirmed by chemical analysis and melting point data is given in Table I.

The ^{1}H-NMR data indicate at $\delta = 8.3$ ppm (2H, br, 2NH), which disappeared on the addition of D_2O due to the proton exchange, $\delta =$ 2.5-2.7 ppm (12H, S, $4CH_3$) and $\delta = 6.9$–7.8 ppm (10H, m, 2Ar).

The therogravimetric analysis (TGA) was measured from room temperature up to 700°C under heating rate 10°C/min. The data were performed using Shimadzu TGA-50 H. The TGA thermograms of ligand and Cu^{+2} complexes indicate two transitions steps and residue due to decomposed products, where the residue is thermally stable up to 700°C, as indicated in Table II, Figure 1. The aminocyclodiphosph(V)azane copper (II) solid complex Scheme 2 of the ligand was prepared by mixing 0.872 g, (0.005 mmol) of the ligand in acetonitrile with 0.223 g (0.01 mmol) of copper bromide. The metal-ligand mixture was refluxed for 3 h, and then kept overnight to separate the

TABLE I Elemental Analyses, Colors, and Melting Points of the Ligand and Cu^{+2} Complex

	Solvent	Yield	M.p.	Chemical formula	Elemental analyses found (Calcd.) %			
Compd.	cryst.	(color)	(°C)	(m.Wwt)	N	S	P	Cu
Ligand	Acetonitrile	89 (Yellow)	208	$C_{26}H_{24}N_{10}S_6P_2Cl_4$ (872.96)	16.00 (16.05)	22.00 (22.05)	7.10 (7.10)	— —
Cu^{+2} complex	Ethanol	94 (Deep violet)	268	$C_{26}H_{24}N_{10}S_6P_2Cl_4Br_4Cu_2$ (1319.39)	10.4 (10.62)	14.30 (14.58)	4.6 (4.70)	9.65 (9.63)

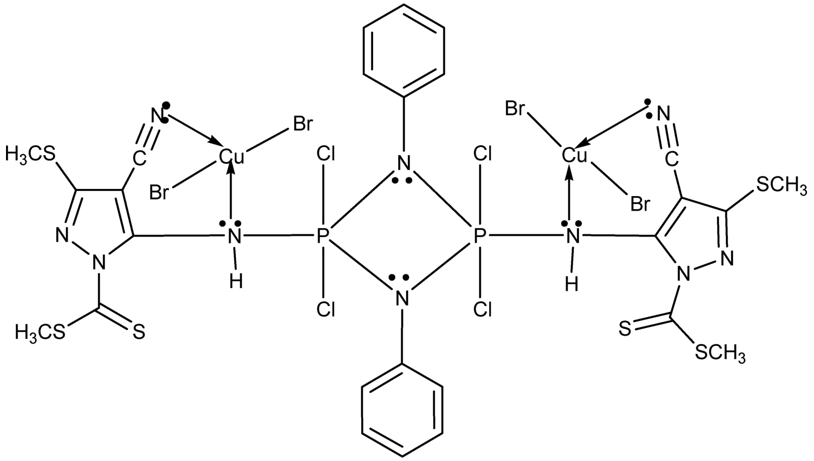

SCHEME 2 Molecular configuration of copper (II) solid complex (1,3-diphenyl-,2,2,,4,4-tetrachloro-bis(5-imino-4-cyano-3-methylthio- pyrazo-1-yl-methylcarbodithioate dibromo copper (II)) cyclodiphosph(V)azane.

copper solid complex. The collected complex was washed several times with acetonitrile to get rid of the excess ligand. The product was dried in vacuo, and its chemical analysis results are shown in Table I. The disappearance of $\delta = 8.3$ ppm due to as an evidence for the ligand formation. The stability constant of the complex is determined potentiometrically as log K = 12.32. Spectral analysis was carried out 28 + 0.1°C using a Shimadzu-IR-440, as KBr – mixed disc, ultraviolet and visible absorption spectra were recorded on a Perkin-Elmer Lambda 3B spectrophotometer. The temperature dependence of dark conductivity was measured utilizing the direct current method, with in 5, 20, and 70 V were within the range of voltage current linearity where Ohm's law is obeyed. The temperature of the samples were measured constant

TABLE II Thermal Analyses Data for the Ligand and Cu^{+2} Complex

(chemical formula) [m.wt.]	Compound Dissociation stages	Temp. range in TG °C	Weight loss found (calcd.)%	Assignment
Ligand	Stage I	360–470	27.80 (27.88)	$C_7H_7N_4S_3$
($C_{26}H_{24}N_{10}S_6P_2Cl_4$)	Stage II	470–700	49.50 (49.99)	$C_{13}H_{12}N_5S_3PCl_2$
[872.69]Cu^{+2}complex	Stage I	330–390	26.00 (26.16)	$C_7H_7N_4PCl_2S_3$
($C_{26}H_{24}N_{10}S_6P_2Cl_4$	Stage II	390–520	21.08 (21.53)	$C_{12}H_{10}N_2PCl_2$
Br_4Cu_2)[1319.39]	Stage III	520–700	52.00 (52.29)	$C_7H_7N_4S_3Cu_2Br_4$

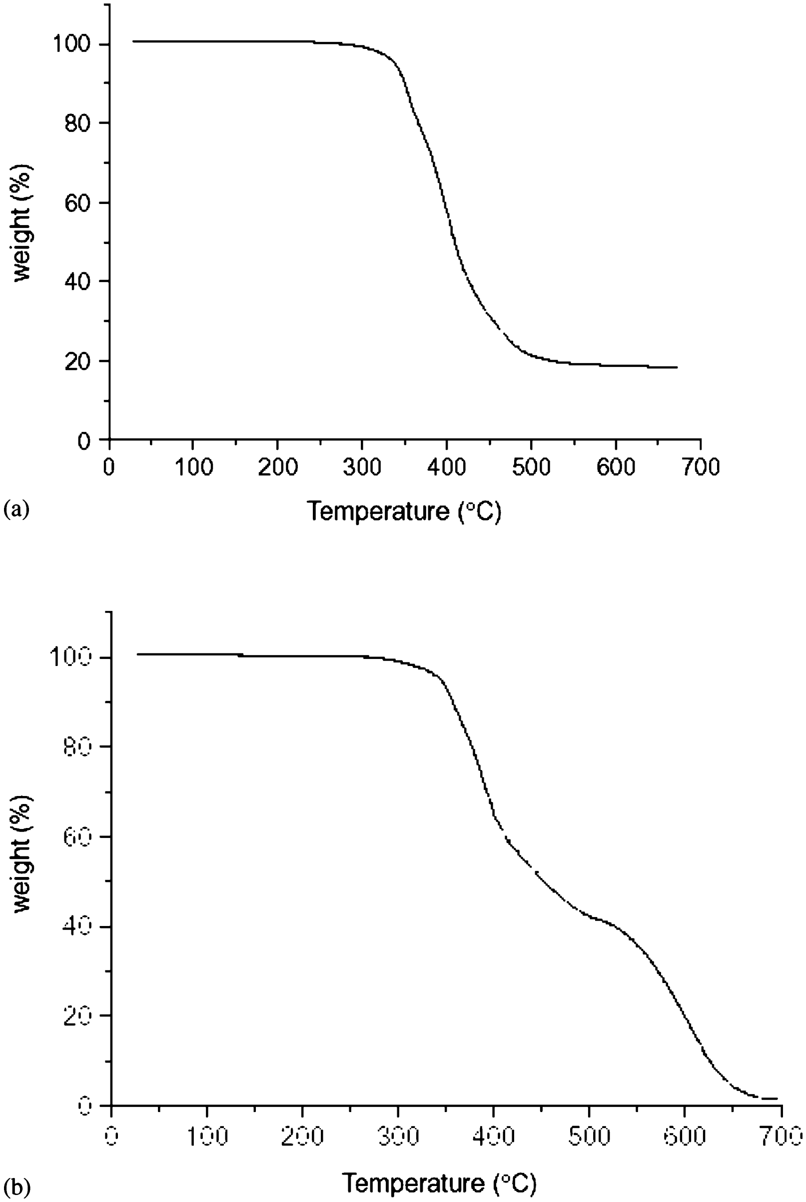

FIGURE 1 Thermogravimetric analysis of a) the ligand and b) Cu(II) complex.

on copper thermocouple placed close to the sample by using the potential probe method.[8] All measurements were performed under atmospheric pressure in presence of nitrogen inert gas. The samples were the form of pellets pressed at 4 tons/cm^2, diameter $\cong$ 10 mm and thickness 1–2 mm, coated with silver paint (BDH) and checked several times for good contact.[9,10] The prepared compounds ligand and its copper complex were checked by thin layer chromatography (TLC) and identified by elemental analysis Table I.

RESULTS AND DISCUSSIONS

DC Electrical Conductivity

The values of dark electrical conductivity (σ) were calculated by using the following equation[11]:

$$\sigma = \mathrm{A}^{-1}\,\mathrm{d}\,\mathrm{V}^{-1}\,\mathrm{I}, \tag{1}$$

where A is the cross-sectional area of the measured surface; d is the thickness of the specimen in the direction of the measurement; A is the voltage applied to the specimen; and I is the measurement current intensity.

The calculation of the activation energy E_A of the charge conduction process of ligand and its Cu^{+2} complex can be determined according to Arrhenius dependence equation:

$$\sigma T = \sigma_0 exp^{(E_A/KT)}, \tag{2}$$

where σ stands for electrical conductivity; σ_0 is a constant; T = absolute temperature; K is the Boltzman's constant; and E is the conduction energy gap.

Figures 2 and 3 show Arrhenius plot for the dark conductivity of ligand, and its copper (II) complex calculations were performed in the inter vales of linearity of the following relationship:

$$\mathrm{Ln}\sigma = \mathrm{f}[1/\mathrm{T}]. \tag{3}$$

The values of the electrical conductivity σ of the compounds under investigation at low and high temperature, the activation energies and appropriate transition temperatures are shown in Table III for ligand (Scheme 1) and its copper (II) complex (Scheme 2).

As expected, the total conductivity of semiconductivity compounds results from both intrinsic and extrinsic conduction and equilibrium change of the molecular structure.

It is therefore, the relation of ln σ vs. 1/T for both ligand and its copper (II) complex yield different lines that depend on ΔE and ΔE_{ex} (where

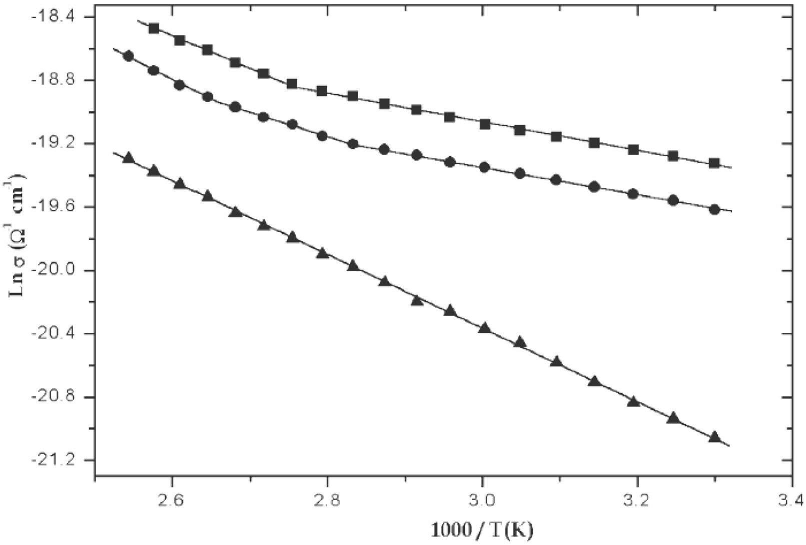

FIGURE 2 The relation between ln σ and reciprocal of absolute temperature 1/T for the ligand at: 5V (■), 20V (•), and 70V (♦).

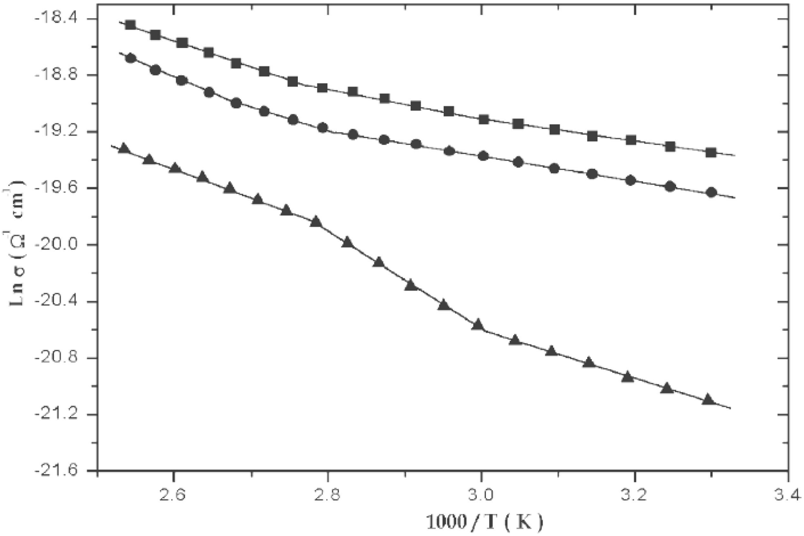

FIGURE 3 The relation between ln σ and reciprocal of absolute temperature 1/T for the copper (II) complex at: 5V (■), 20V (•), and 70V (♦).

TABLE III Values of the Electrical Conductivity (σ) and the Activation Energies E_1, E_{11}, and E_{111} of the Ligand and Cu^{+2} Complex

Compound	Applied voltage (V)	^aT_I (K)	$^aT_{II}$ (K)	^bE_I (low) (eV)	$^bE_{II}$ (eV)	$^bE_{III}$ (high) (eV)	$\sigma_I x10^{-10}$ at 303 K ($\Omega^{-1}cm^{-1}$)	$\sigma_I \times 10^{-9}$ at 393 K ($\Omega^{-1}cm^{-1}$)
Ligand	5	330	382	0.0157	0.0524	0.1209	25.39	3.950
	20	333	373	0.0638	0.0996	0.1387	16.99	3.351
	70	351	386	0.0580	0.2247	0.5239	5.352	1.260
Cu^{+2} complex	5	338	378	0.0458	0.0760	0.1924	7.744	1.282
	20	349	382	0.0704	0.1203	0.2221	4.487	0.850
	70	362	388	0.0931	0.1924	0.4123	2.455	0.492

ΔE_D or $\Delta E_A < \Delta E$),ΔE is the energy gap width, ΔE_A acceptor valence band separation, and ΔE_D is the donor conduction band and separation.

As shown from Figures 2 and 3, the ln σ vs. 1/T plot shows three regions of conduction, which may be (a) region of greater ΔE, (b) region of defect exhaustion and (c) region of lower ΔE. The conductivity of ligand at applied voltage 5 V shows a greater ΔE, which may be due to presence of different structure form the molecule in equilibrium, while at high temperature and higher applied voltage the structure of the molecule exists mainly in the planar form structure which assists in increase the conductivity and decrease in the energy gap (lower ΔE) of the total system in the ligand. Also, the presence of a large number of sulfur atoms in the molecule ligand with large number of nitrogen atoms or due to the great numbers of lone pairs of electrons in the molecule assist in increasing the conductivity of the molecule as given in good semiconducting materials, while the copper complex exist mainly in the planar form of the molecule. So that at all applied voltage the energy gaps approximately the same. The planar form of the molecule all the phenyl rings and other rings lie in the same plane while at higher energy gaps at least two phenyl rings attached to the nitrogen atoms rotate perpendicular to the plane which decrease the conductivity of the molecule or increase the energy gap width of molecule due to the change of molecular structure.

This is also ascribed to the high conjugation that increases the delocalized π electrons along the molecule frame and decreases the energy gap between the ground state and the nearest allowed excited state, as well as increasing the basicity of the nitrogen atom of the amino group to some extent, which participates in the conduction processes in the temperature range of measurements. Data of the electronic absorption spectral analysis also provide support for the mechanism of conduction process taking place in the ligand and its copper (II) complex. The calculated energy gaps corresponding to the maximum absorption wavelength in ultraviolet region in ligand λmax 234 nm, 274 nm and its copper (II) complex (λmax 234 nm, 266 nm, and 325 nm) which corresponds to (5.35, 4.54 eV) and (5.31, 4.67, and 3.82 eV) respectively have been confirmed the observed two pathways conduction processes in both. They are due to the generation of changes of all allowed n-π^* electronic transitions of the lowest excited energy states at low temperature range, which participate in the first stage of conduction. On the other hand, the admixed electrons of the n-π^* and $\pi - \pi^*$ transition contribute in second stage of conduction processes at higher temperature phase.

AC Electrical Conductivity

The AC electrical conductivity properties of samples were measured and were given in Figure 4. The obtained results can be interpreted as follows. The total frequency dependent conductivity $\sigma_{(\omega)}$ can be shown to be the sum of two contributions[12]:

$$\sigma(\omega) = \sigma_0 + \sigma_{\mathrm{AC}}(\omega), \tag{4}$$

where σ_0 is DC conductivity which is independent from frequency; and $\sigma_{\mathrm{AC}}(\omega)$ the AC conductivity increasing with frequency. It is seen from Figure 4 that AC conductivity is almost universal for these samples, and the conductivity plots of samples exhibits three components. The low frequency plateau characterizes the DC conductivity, which corresponds to an unambiguous measurement of DC conductivity and reflects precisely the same temperature dependence. We have also observed the presence of a plateau followed by maximum of conductivity. The same shape of this spectrum is observed in two samples. With regard to the second component, the AC conductivity increases with increasing frequency according to the equation[13]:

$$\sigma_{\mathrm{AC}} = \mathrm{A}\omega^n, \tag{5}$$

where A is a temperature-dependent parameter; and na temperature-independent parameter between 0 and 1. By applying a non-linear least squares computer program, the results were fitted to Equation (5) in the high frequency region. The dependency of conductivity to frequency was detected as $\omega^{0.91\&0.96}$ for ligand and Cu(II) complex, respectively, by fitting conductivity-frequency graphs of samples shown in Figure 4. This can be explained as transport takes place by carriers excited into localized states at the edges of the valence or conduction band. So, electrical charge transport occurs with hopping conduction and the conductivity to increase with frequency approximately as ω.$^{0.91-0.96.}$[13]

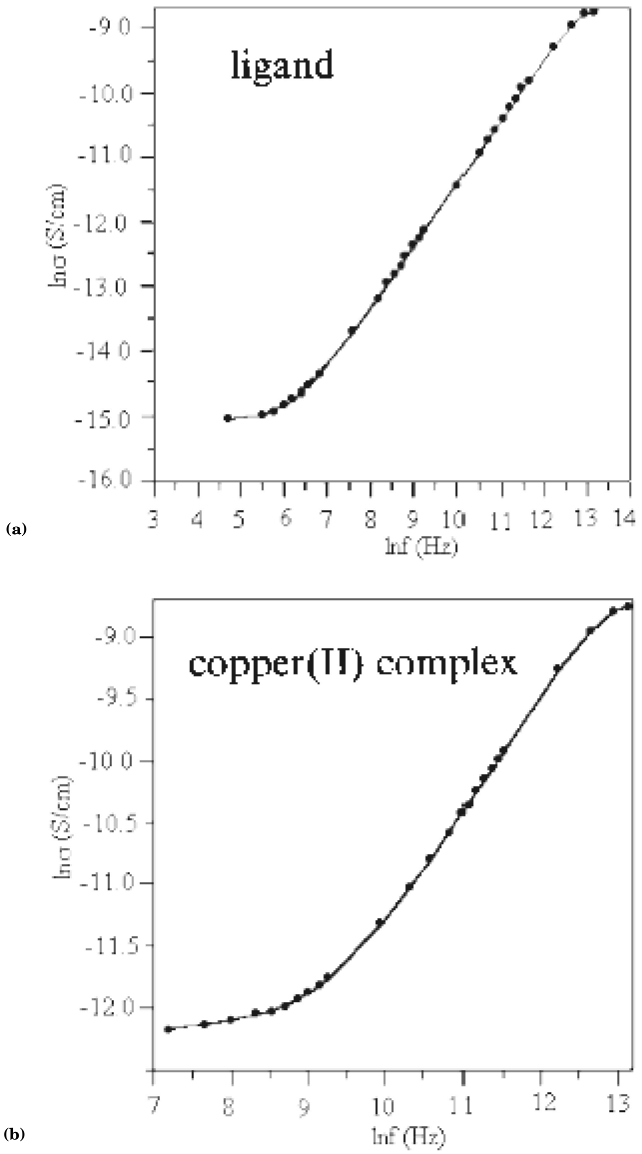

FIGURE 4 The conductivity dependence of frequency of a) ligand (above) and b) Cu(II).

TABLE IV Infrared Spectra of the Ligand and Cu^{+2} Complex

Compound	ν_{NH}	ν_{P-NH}	$\nu_{C\equiv N}$	ν_{P-N}	ν_{P-Cl}	ν_{M-N}	ν_{CH}	ν_{M-Br}
Ligand	3200(br)	2600(w)	2218(s)	1230(m)	524(m)	—	2922(m)	—
Cu^{+2}complex	3152(br)	2600(w)	2208(m)	1215(m)	513(m)	418(m)	2947(m)	530(m)

Infrared Spectra

The assignments of the important bands of the free ligand are given in Table III. The spectra reveal the characteristic bands of the ν_{P-NH} stretching vibrations of the ligand at 2600 cm^{-1}, which is similar to those assigned by Abd-Ellah[14] and Pustinger.[15] The band appeared at 3300 cm^{-1} is attributed to the ν_{NH} stretching vibration. The band observed at 2218 cm^{-1} is ascribed to the $\nu_{C\equiv N}$ stretching vibration which appeared at 2190 cm^{-1} [16] in compound II. The shift of this band to higher frequency in all the ligands is considered as an evidence for the ligand formation. ν_{P-Cl} stretching vibrations are observed at 524 cm^{-1}.[17,18] The band at 1230 cm^{-1} was assigned to the ν_{P-N} stretching vibrations.[19] Bands in the range 1456–1558 cm^{-1} may be attributed to $\nu_{C=C}$ of the aromatic rings and attached compound (II). Moreover, the IR spectra showed weak bands at 650 cm^{-1} due to the ν_{C-S} stretching vibration of pyrazole rings. Two bands at 2980 and 2870 cm^{-1} are assigned to the saturated ν_{C-H} and ν_{C-C} of the pyrazole rings. The weak band observed at the 3120 cm^{-1} is due to aromatic ν_{C-H} stretching vibrations.[14] The most characteristic infrared spectral bands of the metal chelates together with those of the free ligand are collected in Table IV. The IR spectral copper (II) complex show a shift to lower frequencies of both ν_{NH} and $\nu_{C\equiv N}$, indicating that both of the NH and C≡ N groups coordinate via nitrogen atoms metal cations Table III. In copper complex, there are new medium to weak bands appeared at lower frequencies between 418 cm^{-1} is assigned to ν_{M-N} and 530 cm^{-1} was assigned to ν_{M-Br} respectively.[14] The characteristic corresponding to the ν_{P-NH}, ν_{P-N} and ν_{P-Cl} which were associated with all the investigated complexes are collected in Table IV.

The obtained data are in good agreement with those calculated for the suggested structure of the prepared compounds aminocyclodiphossph(V)azane ligand and aminocyclodiphosph(V)azane Cu (II) complex.

The TGA thermograms of aminocyclodiphosph(V)azane ligand and aminocyclodiphosph(V)azane compounds indicate two transition steps and residue due to decomposed products, where the residue is thermally stable up to 700°C as indicated in Table II and Figure 1.

CONCLUSION

Materials with pronounced semiconductive behaviors such as the compounds of this study contribute a number of important perspectives in the solid-state physics and microelectronic fields. The primary objective of our paper has been to explore how the electric conductivity depends on the specific molecular structure. Technically these compounds are considered as semiconductors on the basis of the above deductions.

REFERENCES

[1] S. M. Shaaban, B. A. El-Sayed, A. A. Shabana, and A. M. Hassan, *Materials Letters*, **21,** 255 (1994).
[2] M. A. Ahmed, B. A. El-Sayed, M. M. El-Desoky, and S. M. Shaaban, *Thermochimica Acta*, **168,** 25 (1990).
[3] B. A. El-Sayed, S. M. Shaaban M. M. El-Desoky, and M. A. Ahmed, *J. of Materials Science: Materials in Electronics*, **2,** 11 (1990).
[4] B. A. El-Sayed, M. M. El-Desoky, S. M. Shaaban, and M. B. Sayed, *J. of Materials Science: Materials in Electronics*, **3,** 124 (1992).
[5] M. M. Sallam, B. A. El-Sayed, and S. M. Shaaban, *J. of Materials Science: Materials in Electronics*, **10,** 1–4 (1999).
[6] A. M. A. Alaghaz, Ph. D. Thesis, Faculty of Science(Boys), Al-Azhar University, Cairo, Egypt 2004.
[7] R. S. Farag, I. M. Abd-Ellah, S. M. Shaaban, B. A. El-Sayed, and A. M. A. Alaghaz, *Al-Azhar Bull. Sci.,* **15,** 283–292 (2004).
[8] M. A. Ahmed and F. A. Radwan, *J. Phys. Chem. Solids*, **49,** 385 (1988).
[9] L. Kubisz and E. Marzec, *J. of Non-Crystalline Solids*, **305,** 322 (2002).
[10] D. E. Hill and J. E. Katon, Ed., *Organic Semiconducting Polymers* (Marcel Decker, New York, 1968), p. 3.
[11] M. H. Shamos and J. Zipkin, Ed., *Biological Mineralzation*, (Wiley, New York, 1973), p. 363.
[12] P. Dutta, S. Biswas, M. Ghosh, S. K. De, and S. Chatterjee, *Synth. Met.,* **122,** 455 (2001).
[13] N. F. Mott and E. A. Davis, *Electronic Processes in Non-Crystalline Materials* (Clarendon Press, Oxford, 1979).
[14] I. M. Abd-Ellah, B. A. El-Sayed, M. A. El-Nawawy, and A. M. A. Alaghaz, *J. Phosphorous, Sulfur, and Silicon*, **177,** 2895 (2002).
[15] J. V. Pustinger, W. T. Cave, and M. L. Neilsen, *Spectrochim. Acta*, **15,** 909 (1959).
[16] T. Tomingo, T. Honkawa, M. Hora, and A. Hosomi, *J. Heterocyclic Chemistry*, **27,** 775 (1990).
[17] D. E. C. Corbridge, *J. Appl. Chem. (London)*, **6,** 456 (1956).
[18] L. C. Thoams and R. A. Chittenden, *Chem. Ind. London*, 1913 (1961).
[19] R. B. Harvey and J. E. Mayhood, *Can. J. Chem.,* **33,** 1552 (1955).